

# Correlating galaxy morphologies and spectra in the 2dF Galaxy Redshift Survey

Darren S. Madgwick\*

*Institute of Astronomy, Madingley Road, Cambridge CB3 0HA, U.K.*

Accepted 2002 September 3. Received 2002 June 7; in original form 2002 April 14

## ABSTRACT

The correlation between a galaxy’s morphology and its observed optical spectrum is investigated. As an example, 4000 galaxies from the 2dF Galaxy Redshift Survey, which possess both good quality spectra and have visually determined morphologies are analysed. Of particular use is the separation of Early and Late type galaxies present in a redshift survey since these can then be used in their respective redshift-independent distance estimators ( $D_n - \sigma$  and Tully-Fisher). It is determined that galaxies in this sample can be relatively successfully separated into these two types by the use of various statistical methods. These methods are briefly outlined in this paper and are also compared to the default 2dFGRS spectral classification  $\eta$ . In addition it is found that the 4000Å break in the spectrum is the best discriminant in determining its morphological type.

**Key words:** methods: statistical – galaxies: elliptical and lenticular, cD – galaxies: spiral

## 1 INTRODUCTION

The classification of galaxies according to their observed morphologies has proved to be a very useful way of characterising different galaxy populations (see e.g. Hubble 1936). However, the high-resolution imaging data required to make such accurate morphological classifications, over a wide range of redshifts, is often unavailable in large galaxy redshift surveys. In this paper, a selection of different statistical methods are investigated, with the aim of establishing a quantifiable link between a galaxy’s morphology and its observed optical spectrum; thousands of which are now available through the advent of large galaxy redshift surveys such as the Sloan Digital Sky Survey (York et al. 2000) and the 2dF Galaxy Redshift Survey (2dFGRS, Colless et al. 2001). In particular, a set of 4000 galaxies which have already been observed in the 2dFGRS, for which the morphology and spectrum have been determined, is used as a training set. It has long been established that a substantial link exists between the overall structure of a galaxy and the chemical properties reflected in its spectrum - which quantifies its stellar and gas composition (e.g. Morgan & Mayall 1957). However, efforts to quantify this relationship have been somewhat hampered due to the lack of large, representative, data-sets. For example, Folkes, Lahav & Maddox (1996) used a sample of only 26 unique galaxy spectra and morphologies in a similar analysis to that presented here. This is fortunately no longer an issue with the advent of fibre-based galaxy redshift surveys, which are able to acquire several hundred galaxy spectra per hour.

These surveys are producing extremely large data-sets for which the spectrum of a galaxy is known but its detailed struc-

tural parameters generally are not, or are very difficult to determine accurately from the photometry of the input catalogue over a representative redshift range. Fortunately, the spectrum of a galaxy is generally a more robust quantity to measure over a variety of redshifts and as such if a substantive link between optical spectra and these parameters can be determined this will greatly enhance our ability to probe the properties of our local galaxy population.

Another more specific advantage of being able to determine a galaxy’s morphology from its spectrum is that it allows the identification of targets for peculiar velocity follow-ups (using either  $D_n - \sigma$  for elliptical galaxies or the Tully-Fisher relation for spirals).

In this paper two statistical techniques are investigated, to determine how accurately morphology can be estimated from a galaxy’s optical spectrum. Both methods are ‘supervised’ - meaning that they require a training set of galaxies with both visually determined morphologies and observed spectra. The first method to be implemented is Fisher’s linear discriminant (Section 4), which attempts to determine an optimal linear combination of inputs (the spectrum) to distinguish between several outputs (the morphologies). The second method is an Artificial Neural Network (ANN, Section 5) which creates non-linear combinations of the input, and outputs a selection of class probabilities. The possible biases introduced into this work by systematic effects are described in Section 6 and then the success rates of each method are compared to those achieved using the default 2dFGRS spectral classification parameter,  $\eta$ , in Section 7.

\* E-mail: dsm@ast.cam.ac.uk (DSM)

## 2 GALAXY MORPHOLOGIES IN THE 2DFGRS

A number of galaxies in the 2dFGRS have already had their morphologies determined manually by direct examination of the APM Galaxy Survey images (Maddox et al. 1990a,b see Fig. 1). The accuracy and completeness of this sample varies a great deal depending on the source of the classification and the range of galaxy magnitudes considered. In what follows I primarily make use of those galaxies which were ascribed morphologies in the APM Bright Galaxy Catalogue (Loveday 1996). This catalogue provides a complete sample of classified galaxies down to a magnitude limit of  $b_J = 16.44$ . The exact value of this magnitude limit now varies across the sky due to recent re-calibrations of the APM magnitudes (see e.g. Colless et al. 2001 for details of the most recent calibrations of those galaxies included in the 2dFGRS), however this will not have any substantial impact upon the representativeness of our classified sample. A significant number of galaxies at fainter magnitudes also have morphologies determined from other sources, but these will be substantially less reliable and so are not used in this analysis.

Of those  $b_J < 16.5$  galaxies which have been successfully observed so far in the 2dFGRS, 3899 have a morphological classification (Fig. 2). The galaxy morphologies are given in four broad bins: Elliptical, S0, Spiral and Irregular. However, in the analysis presented here they are rebinned into only two classes; Early (Elliptical,S0) and Late (Spiral,Irregular) types. The reasons for doing so are two-fold: Firstly, the number of classified galaxies which have been identified as S0 or Irregular are significantly smaller than the number of Spirals. Therefore the identification of these types will be greatly hindered by the presence of Spiral outliers - which effectively swamp out any identifying signal which may arise from these types. Secondly, the distinction between Early and Late type galaxies is of fundamental importance to observational cosmology since each can be used in its own redshift-independent distance estimator, i.e.  $D_n - \sigma$  for Early types (Dressler et al. 1987) and the Tully-Fisher relation for Late types (Tully & Fisher 1977).

Note that this sample of galaxies consists entirely of relatively bright, nearby galaxies and so may not be representative of the entire 2dFGRS galaxy population. Another important point to bear in mind is that as these galaxies are relatively extended on the sky, the spectra observed of them (through the fixed fibre aperture of the 2dF instrument) may not be representative of the entire galaxy. This so called ‘aperture effect’ is a difficult issue to address and has led to much discussion in the literature (see e.g. Kochanek, Pahre & Falco, 2000; Madgwick et al. 2002). The possible impact of aperture effects on our results is discussed further in Section 6.

## 3 GALAXY SPECTRA IN THE 2DFGRS

The purpose of this analysis is to relate the spectrum of a galaxy to its morphology. In the case of the 2dFGRS each spectrum consists of 1024 channels spanning the wavelength range of approximately 3700-8000Å, thereby including all the major optical diagnostics between O[II] and H $\alpha$  (see Folkes et al. 1999, for further details). As an illustration, the average 2dFGRS spectrum for a representative volume-limited sample is shown in Fig. 3.

Rather than dealing with all 1024 spectral channels in the subsequent analysis (to represent a given spectrum), it is possible to take advantage of the fact that the vast majority of these channels are redundant by means of some form of data compression. In the analysis presented here use is made of a Principal Component

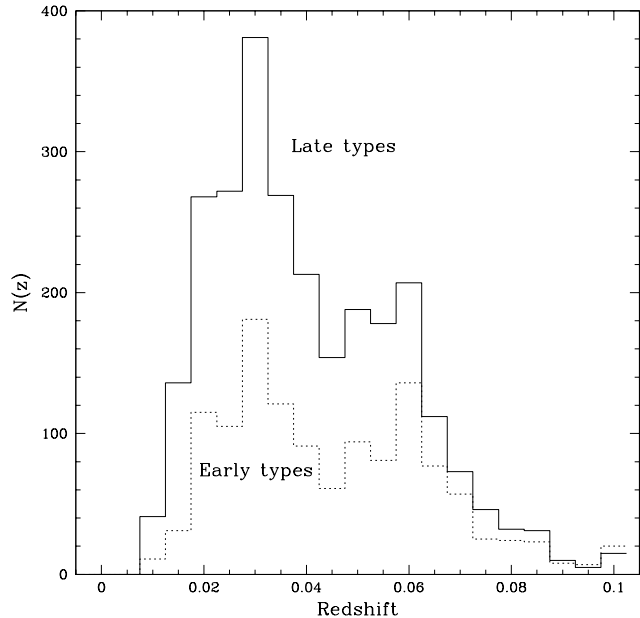


**Figure 2.** The distribution of redshifts of those galaxies classified as Early or Late in the 2dFGRS. Note that in order to ensure that the classification is relatively robust we only include those galaxies within the magnitude limit  $b_J < 16.5$ .

Analysis (PCA, see e.g. Murtagh & Heck 1987) since this compression algorithm has met with considerable success in dealing with galaxy spectra (e.g. Connolly et al. 1995; Galaz & de Lapparent 1998; Folkes et al. 1999; Madgwick et al. 2002).

### 3.1 Review of PCA

PCA is a well established statistical technique which has proved very useful in dealing with high dimensional data sets. In the particular case of galaxy spectra we are typically presented with approximately 1000 spectral channels per galaxy, however when used in applications this is usually compressed down to just a few numbers, either by integrating over small line features - yielding equivalent widths - or over wide colour filters. The key advantage of using PCA in our data compression is that it allows us to make use of all the information contained in the spectrum of a galaxy in a statistically unbiased way, i.e. without the use of such ad hoc filters.

In order to perform the PCA on our galaxy spectra we first construct a representative volume limited sample of the galaxies. When we apply the PCA to this sample it constructs an orthogonal set of components (eigenspectra, herein denoted  $PC_1, PC_2, etc$ ) which span the wavelength space occupied by the galaxy spectra. These components have been specifically chosen by the PCA in such a way that as much information (variance) is contained in the first eigenspectrum as possible, and that the amount of the remaining information in all the subsequent eigenspectra is likewise maximised. Therefore, if the information contained in the first  $n$  eigenspectra is found to be significantly greater than that in the remaining eigenspectra we can significantly compress the data set by swapping each galaxy spectrum (described by 1000 channels) with just those first  $n$  projections (denoted  $pc_1, pc_2$  etc). The variances corresponding to the first 10 principal components derived in this manner are shown in Table 1.

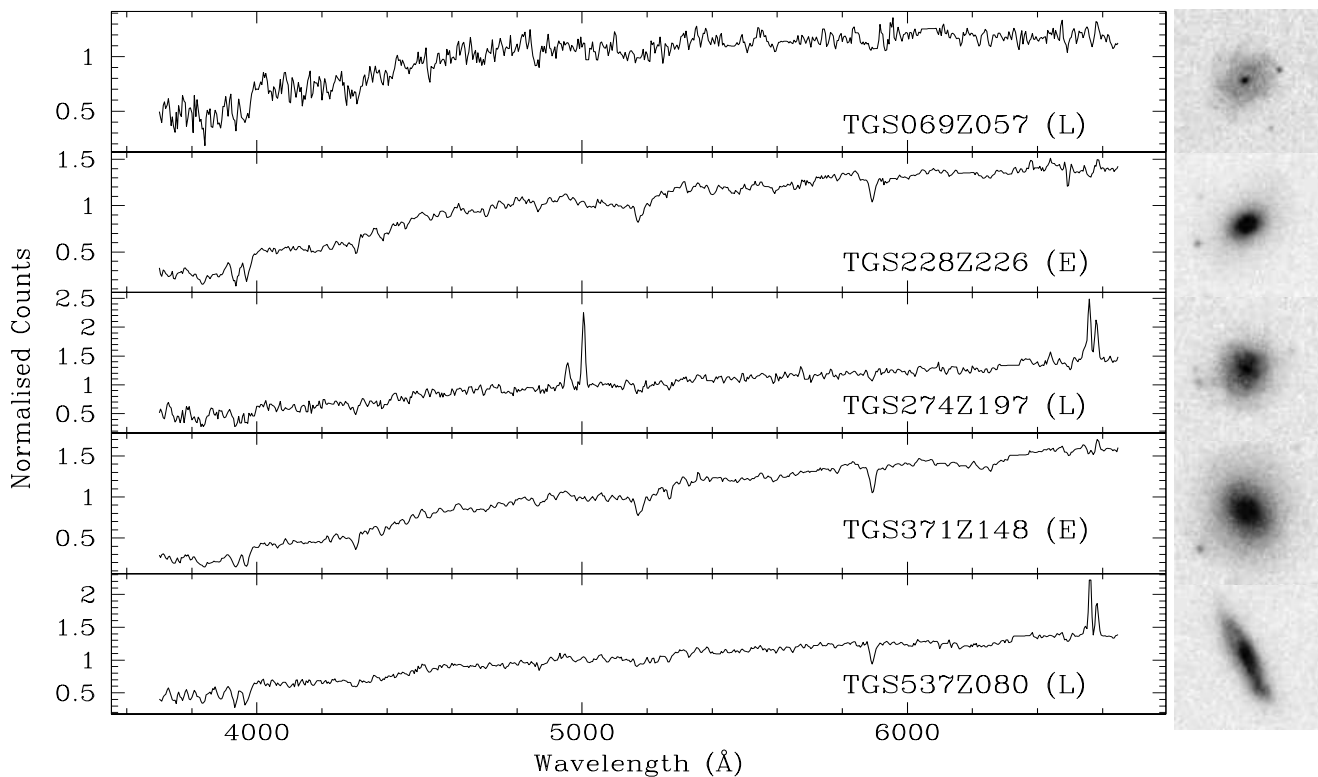


**Figure 1.** A selection of example galaxy spectra and images are shown. The spectra have been taken from the 2dF Galaxy Redshift Survey and are in units of counts/bin with arbitrary normalisation. The images shown are  $1 \times 1$  arcmin postage stamps, in the standard astronomical orientation, taken from the SuperCOSMOS Sky Survey (Hambly et al. 2001). For each spectrum the 2dFGRS object name is given and the labels (L) and (E) refer to Late-type and Early-type morphologies respectively.

**Table 1.** Variance contained in the first 10 principal components of the 2dFGRS galaxy spectra.

Component	Variance (%)	Component	Variance (%)
1	54	6	0.99
2	15	7	0.86
3	4.0	8	0.57
4	2.7	9	0.41
5	1.2	10	0.27

Note that the PCA is merely a statistical tool, we do not imply (yet) that any of these components are physically significant, but rather we are merely using them as a method of data compression.

During the PCA analysis it was found that the eigenspectra became dominated by unphysical broad features from the fifth eigenspectrum ( $\text{PC}_5$ ) onwards. This was due to artifacts from sky emission features which we were unable to completely remove during the spectral reduction. Rather than restrict our future analysis to only the first four principal components, we have instead repeated the analysis with the wavelength range 5850-6200Å masked out. This has no noticeable effect on the original first four eigenspectra, all of which are essentially identical between the two PCA implementations. However, it does allow us to probe deeper into the PCA space than we would otherwise have been able to (up to  $\text{PC}_9$ ).

It is worth noting that most galaxy spectra can be accurately

reconstructed using only the first 4-5 principal components. In our subsequent analysis we make use of the first nine (this choice is justified in detail by Folkes, Lahav & Maddox 1996).

In order to gain some initial understanding of the link between galaxy spectra and morphologies, histograms are shown in Fig. 4 of the distributions of principal component projections for both Early and Late type galaxies. Also plotted are the eigenspectra for each of these projections, which illustrate what spectral features are encoded in the respective projections (Fig. 5). Included in each of these plots are the corresponding results for the  $\eta = 0.5pc_1 - pc_2$  projection which is used to spectrally classify the 2dFGRS galaxies (see next Section). It can be seen that most of the first nine principal components encode some degree of information about the morphology of a galaxy, although none are capable of separating Early from Late type galaxies accurately (with the exception of the  $\eta$  spectral classification). The aim of the analysis presented in this paper is essentially to determine if it is possible to improve the separation between Early and Late types by taking either linear (Fisher Analysis, Section 4) or non-linear (Artificial Neural Networks, Section 5) combinations of these projections.

### 3.2 Spectral classification in the 2dFGRS

The 2dF instrument (Lewis et al. 2002) was designed to measure large numbers of redshifts in as short an observing time as possible. However, in order to optimise the number of redshifts that can

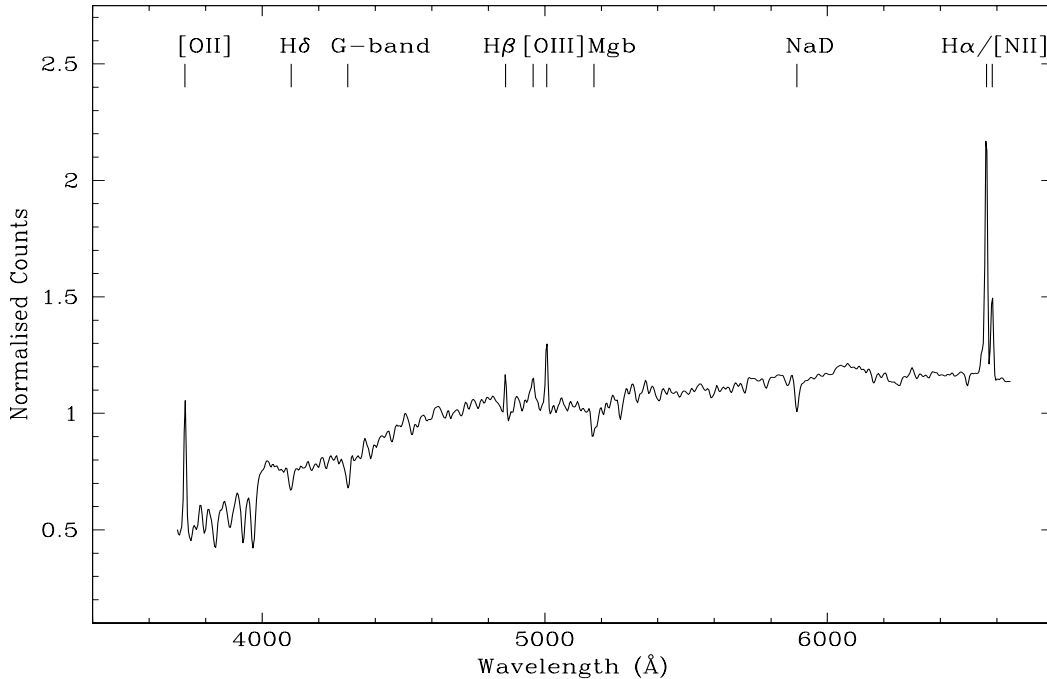


**Figure 3.** The average spectrum of an  $M_{b_J} - 5 \log_{10}(h) > -18$  volume-limited sample of galaxies drawn from the 2dF Galaxy Redshift Survey. The main spectral features present are labelled.

be measured in a given period of time, compromises have had to be made with respect to the spectral quality of the observations. Therefore if one wishes to characterise the observed galaxy population in terms of their spectral properties care must be taken in order to ensure that these properties are robust to the instrumental uncertainties.

The quality and representativeness of the observed spectra can be compromised in several ways and a full list is presented in previous work (see e.g. Madgwick et al. 2002). The net effect is that the uncertainties introduced into the fibre-spectra predominantly affect the calibration of the continuum slope and have relatively little impact on smaller-scale features such as the emission/absorption line strengths. For this reason any given galaxy spectrum which is projected into the plane defined by  $(pc_1, pc_2)$  will not be uniquely defined in the direction of varying continuum but will be robust in the orthogonal direction (which measures the average line strength, see Fig. 6).

The projection onto this robust axis is denoted by  $\eta$  (ETA\_TYPE in the 2dFGRS catalogue<sup>1</sup>),

$$\eta = a \cdot pc_1 - pc_2. \quad (1)$$

Where  $a$  is a constant which we find empirically to be  $a = 0.5 \pm 0.1$ . This (continuous) variable  $\eta$ , being the single most important component of the galaxy spectra which was robust to instrumental uncertainties, was chosen as the measure of spectral type in 2dFGRS.

Note that although  $\eta$  is a continuous measure of type, it is often useful to divide a galaxy sample into different bins to simplify subsequent analyses. One of the most common divisions to make

is to separate those galaxies with  $\eta < -1.4$  from those with  $\eta \geq -1.4$ , referred to as *relatively* quiescent and star-forming galaxies respectively.

#### 4 FISHER'S LINEAR DISCRIMINANT

It is clear from the trends in Fig. 4 that morphology is indeed related to the spectra of galaxies although, with the exception of the  $\eta$  spectral classification, the correspondence is not particularly pronounced. However, as shown by  $\eta$ , it may be possible to improve this situation by taking various linear combinations of the projections in order to isolate those particular parts of a galaxy's spectrum which contain the most information regarding its morphology.

In this section a method first proposed by Fisher (see e.g. Bishop 1995 and references therein) is considered, for linearly reducing data dimensionality (in this case we hope to go from our 9 principal components to 1 morphology) in a way which will optimally distinguish between different classes of objects. Strictly speaking this method will not create a discriminant between the two classes but rather, once we have reduced the dimensionality, it should become clear how to divide the sample.

As mentioned before, this method is a linear approach to this problem. In the next section this will be generalised to consider the possibility of a non-linear relationship between morphology and spectra through the use of Artificial Neural Networks.

##### 4.1 Mathematical formulation

The mathematical formulation of Fisher's linear discriminant is straight-forward. We consider a set of input vectors  $\mathbf{x}$ ; we wish

<sup>1</sup> <http://www.mso.anu.edu/2dFGRS/>

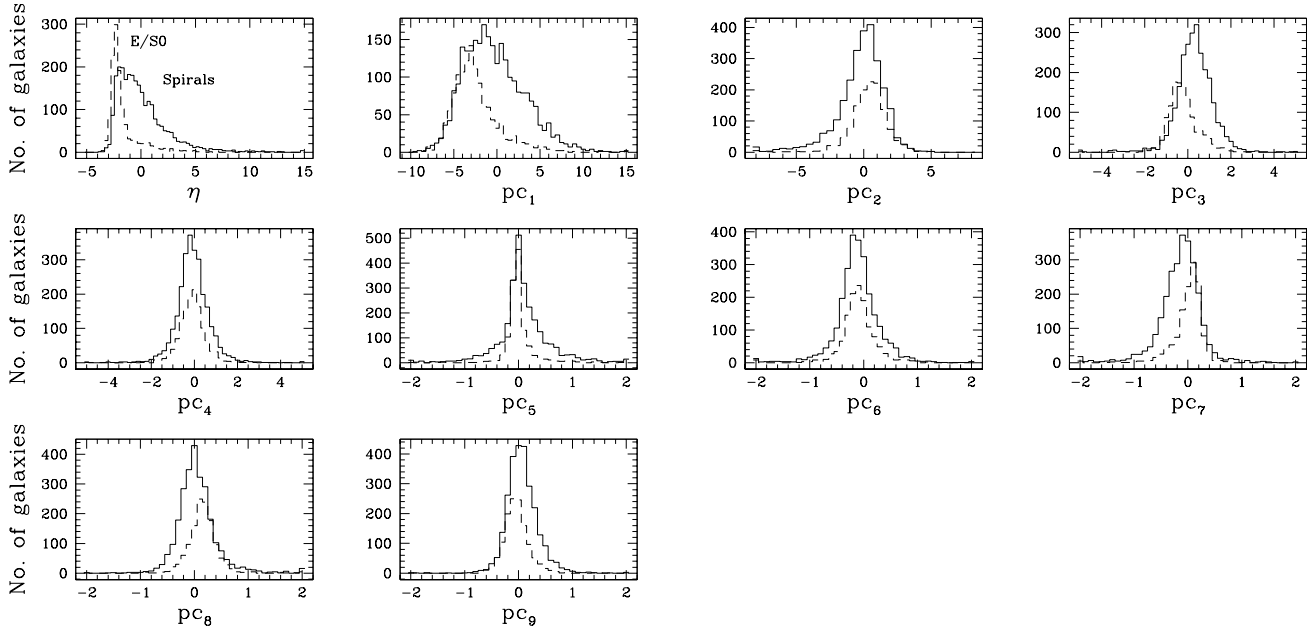


**Figure 4.** The distribution of  $\eta$  for E/S0 (dotted line) and Spiral galaxies (solid line) is shown in the top left panel. The other panels show these distributions for the first 9 principal components.

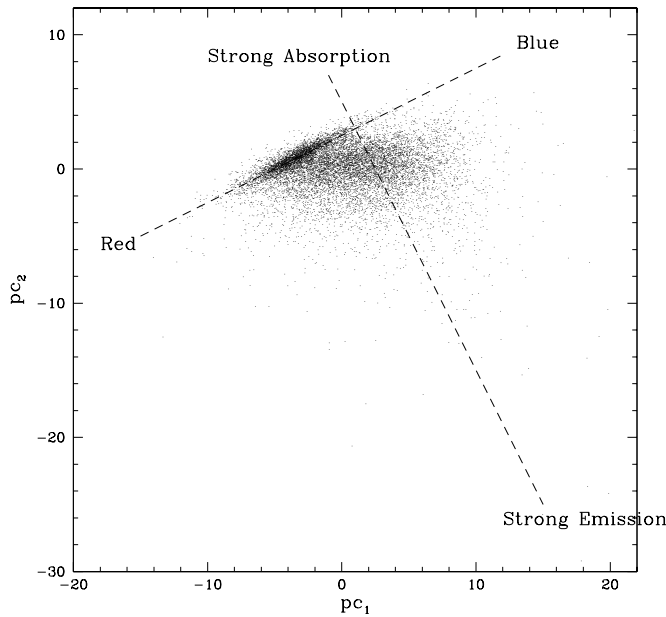


**Figure 6.** The distribution of  $(pc_1, pc_2)$  projections of the observed 2dF galaxies is shown. Also shown are the projections which maximise either the continuum or emission/absorption component in each spectrum. The latter of these projections is used to classify the 2dFGRS galaxies.

to determine the weights  $\mathbf{w}$ , such that the projection  $\mathbf{y}$  is the most discriminatory between our two classes,

$$\mathbf{y} = \mathbf{w}^T \mathbf{x} \quad (2)$$

The mean vectors  $\mathbf{m}_1$  and  $\mathbf{m}_2$  of each class are given by,

$$\mathbf{m}_k = \frac{1}{N_k} \sum_{n \in C_k} \mathbf{x}^n . \quad (3)$$

Here  $n \in C_k$  are the elements of class  $C_k$  (in this case  $k = \{1, 2\}$  for Early and Late types respectively). After projection, the scalar separation between the means will be,

$$m_2 - m_1 = \mathbf{w}^T (\mathbf{m}_2 - \mathbf{m}_1) , \quad (4)$$

and the *within-class* covariance is,

$$s^2 = \sum_{n \in C_k} (y^n - m_k)^2 \quad (5)$$

Fisher's assertion was that the optimal mapping to be used in reducing our dimensionality should be such as to maximise,

$$J(\mathbf{w}) = \frac{(m_2 - m_1)^2}{s_1^2 + s_2^2} . \quad (6)$$

This is easy to interpret physically: We wish to find a set of weights  $\mathbf{w}$  such as to maximise the mean separation between the two classes  $(m_2 - m_1)$  after we have performed our projection. The variance in the denominator takes into account the fact that our initial vectors  $\mathbf{x}$  may have different spreads and hence differing degrees of overlap in different directions. Clearly we wish to find a projection which minimises this overlapping between our two classes.

To determine the optimal weights we simply need to re-introduce the explicit weight dependence into Eqn. 6 and differentiate. It is shown in Bishop (1995) that the solution is then,

$$\mathbf{w} \propto \mathbf{S}_w^{-1} (\mathbf{m}_2 - \mathbf{m}_1) . \quad (7)$$

Where,

$$\mathbf{S}_w = \sum_C \sum_{n \in C} (\mathbf{x}^n - \mathbf{m}_c)(\mathbf{x}^n - \mathbf{m}_c)^T \quad (8)$$

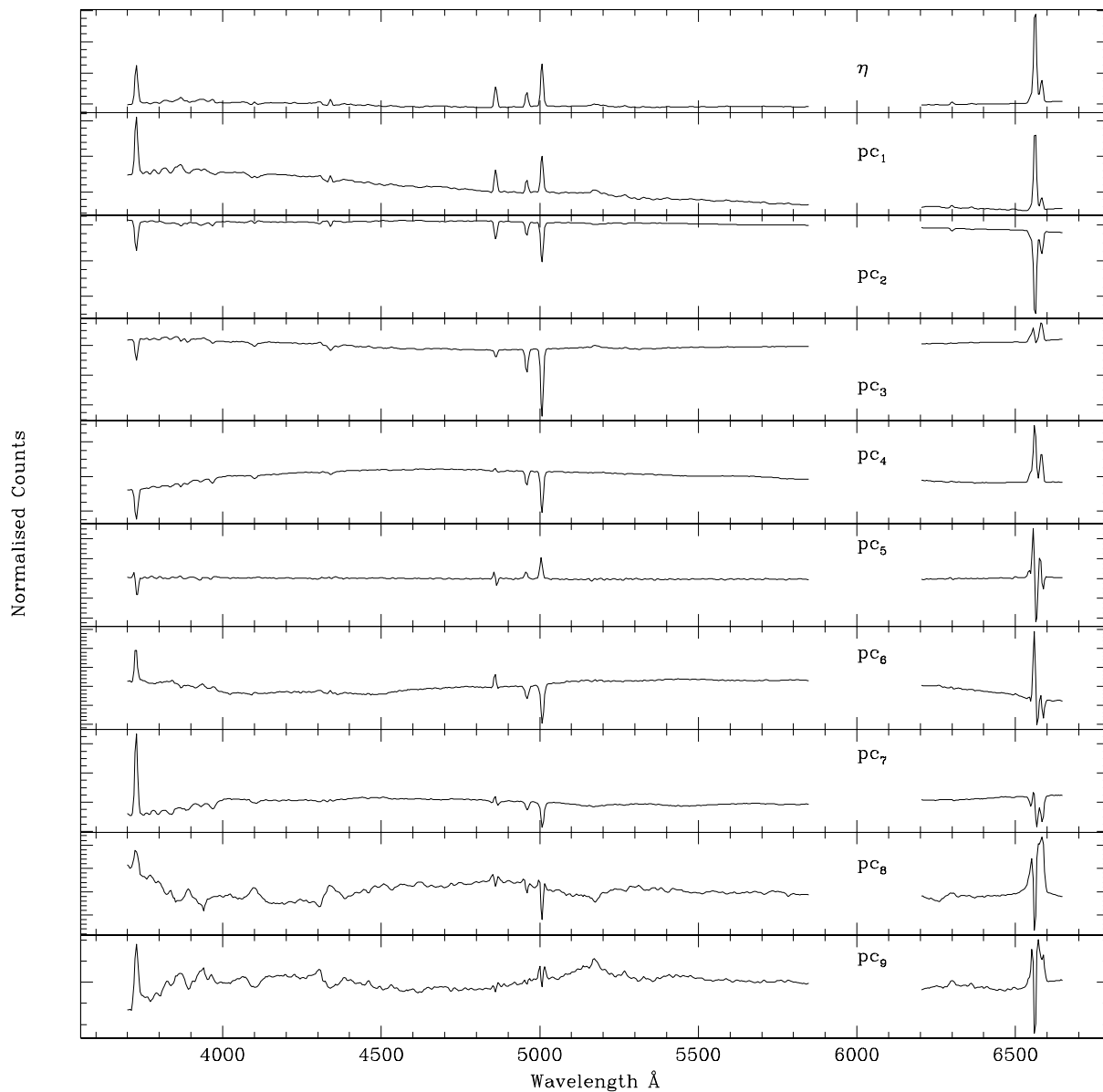


**Figure 5.** The first 9 principal components. Also shown is the spectrum of the  $\eta$  component (top panel), used to classify the 2dFGRS.

is the total *within-class* covariance matrix. Equation 7 only yields the direction of the weight vector, not its magnitude. Conventionally the magnitude of  $\mathbf{w}$  is taken to be such that  $\sum_i w_i^2 = 1$ .

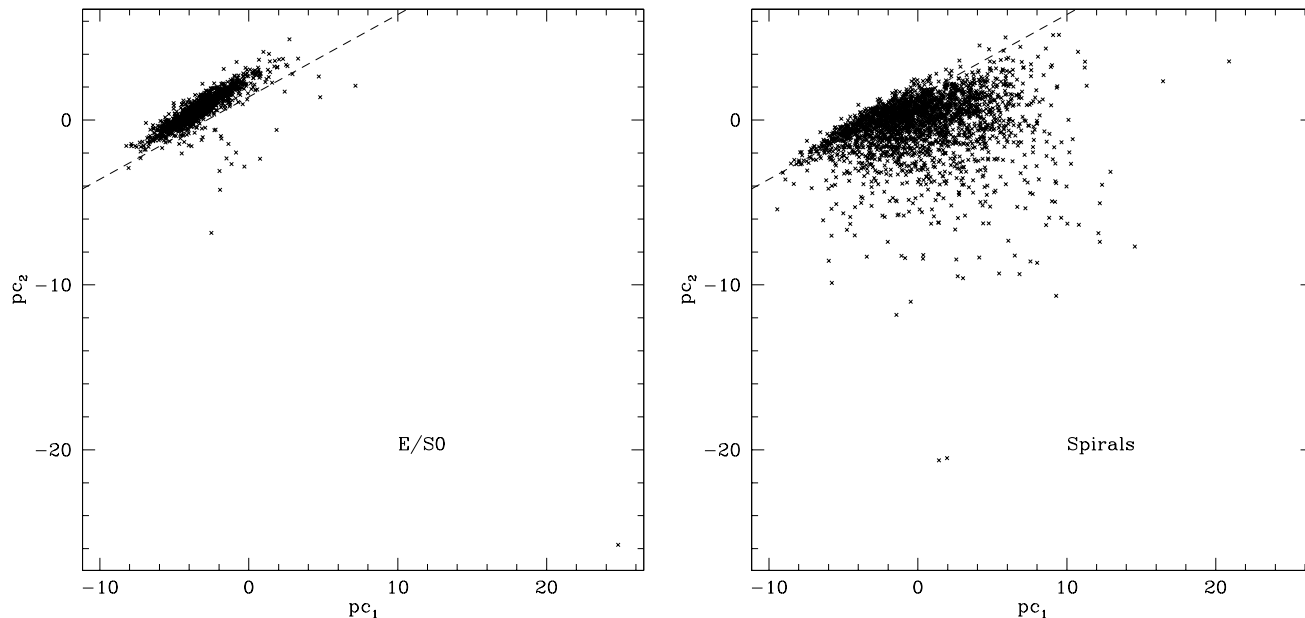
#### 4.2 Classification using the Fisher analysis

After performing the Fisher analysis on the complete set of morphologically classified 2dFGRS galaxies, the resulting weighting vector is found to be,

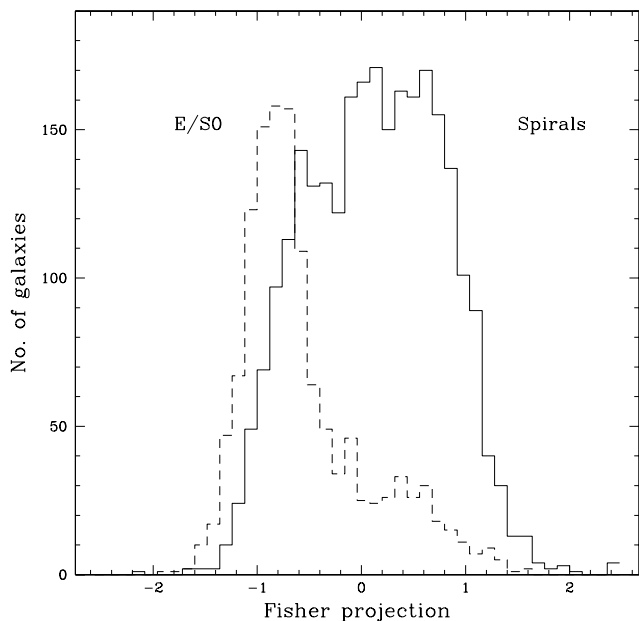
$$\mathbf{w} = (1.2, -1.3, 3.5, 0.18, 0.34, -0.96, -0.68, -6.5, 6.4)/10 .(9)$$

Figure 7 shows the resulting Fisher projections using these weights for both the known Early and Late type galaxies in the 2dFGRS. It is clear from this figure that the method has been relatively successful in that the distinction between Early and Late type galaxies is now much more pronounced than for any of the individual principal components (Fig. 4).

Having derived this projection it is now necessary to determine ‘by-hand’ a cut that we will use to distinguish Early from Late type galaxies in the future. The actual cut adopted will, of course, depend on the specific application for which one requires the galaxies to be classified. For example, if one requires a complete sample of Early type galaxies a relatively high cut should be



**Figure 8.** The  $pc_1$  and  $pc_2$  projections of the morphologically classified 2dFGRS galaxies are shown. Here the morphologies have been derived using Fisher’s method with 9 principal components. It is remarkable that all the information in these 9 components is essentially contained in these first two projections. The Fisher discriminant has been cut at  $-0.55$ .



**Figure 7.** Fisher’s linear discriminant, as calculated from the first nine principal components with the aim of discerning the galaxy morphology. It is clear a significant degree of overlap between the morphological types still exists.

adopted compared to if one requires a relatively ‘pure’ sample. We note that in the context of deriving a pure sample, the results appear to be somewhat disappointing in that the Fisher analysis does not appear to be as discriminatory between Early and Late type galaxies as would otherwise have been hoped.

From Fig. 7 we conclude that a good general distinction between Early and Late type galaxies can be achieved by cutting the distribution at  $-0.55$ . Using this cut gives the total number of galaxies classed Early and Late as  $(814,454)$  and  $(475,2156)$  respectively, where  $(x_1, x_2)$  represents  $x_1$  galaxies that are genuinely Early type and  $x_2$  that are genuinely Late type. Note that the contamination between types will vary substantially depending on the selection criteria of the redshift survey, and so we are primarily interested in the success rates of the classification i.e. 63% of Early types and 82% of Late types successfully classified, as opposed to the degree of contamination.

The distribution shown in Fig. 7 is very similar to that shown in Fig. 4 for  $\eta$ . Indeed, Fig. 8 shows the  $(pc_1, pc_2)$  projections for our sample of galaxies separately, depending on whether they satisfied the Fisher  $-0.55$  criterion for being Early or Late type. Overplotted on this figure is the cut imposed to classify the 2dFGRS into Type 1 (Quiescent) galaxies using  $\eta$  (see Section 3.2). The correspondence is remarkable. Clearly much of the physical information carried in the PCA eigenspectra is contained in the first two principal components. It is also interesting that repeating the Fisher analysis using only these first two principal components yields a classification parameter very similar to  $\eta$  (with very similar success of classification). These two forms of classification (Fisher and  $\eta$ ) are contrasted further in Section 7.

It is worth noting that most spectral classifications are in fact indirectly anchored to morphological types by use of a training set (e.g. the Kennicutt Atlas, Kennicutt 1992) of galaxy spectra for which the morphology is known (see e.g. Connolly et al. 1995; Folkes et al. 1999). However, in the case of the 2dFGRS,  $\eta$  was chosen purely on the grounds of robustness with respect to instrumental uncertainties in determining the spectral continuum. This point is discussed further in Section 7.

### 4.3 Spectral features

If we combine the PCA eigenspectra (Fig. 5) using our derived weighting vector  $\mathbf{w}$  we can determine which spectral features are being used by the Fisher criterion to measure galaxy morphology. This spectrum is shown in Fig. 9.

It must be borne in mind, when attempting to interpret this spectrum, that the PCA is mean-subtracted, i.e. the average 2dF-GRS spectrum has been subtracted from each individual spectrum before calculating its projection (see Fig. 3). Therefore negative values in this eigenspectrum represent either absorption or below average emission, whereas positive values correspond to above average emission.

Perhaps the most striking feature of the spectrum shown in Fig. 9 is its overall lack of nebular emission features, despite the fact that these dominate most of the PCA eigenspectra (see Fig. 5). It is interesting that this spectrum, which is so clearly different to that used to calculate  $\eta$  (see top panel of Fig. 5), should give such a similar classification. Clearly there is a very pronounced correlation between the nebular emission features used to calculate  $\eta$ , and the strength of the 4000Å break and (to a lesser degree) the H $\alpha$  emission line, as measured by this combined eigenspectrum. The apparent broad feature at 5200Å (corresponding to the Mgb absorption line) is an artifact introduced due to our truncating the series of eigenspectra just as this feature was becoming prominent in them (it can be clearly seen in  $\mathbf{PC}_8$  and  $\mathbf{PC}_9$  in Fig. 5), and as such this is not contributing to the success of the classification itself.

In fact it is possible to determine more accurately exactly what parts of this spectrum are being used by the Fisher criterion to determine morphology by ‘masking-out’ certain segments of the combined eigenspectrum of Fig. 9, and then seeing how accurately one can recover the same classification (after re-projecting the galaxy spectra onto it). By doing this it can be shown that the entire classification is based on the part of the eigenspectrum below 4800Å, and hence that the morphology of a galaxy can be most accurately determined from the size of the 4000Å break, without the use of any further spectral information (although using the entire spectrum does not degrade the result, and hence will continue to be used throughout this work).

## 5 ARTIFICIAL NEURAL NETWORKS

This section further refines the analysis of the previous section by considering the possibility of a nonlinear relationship between a galaxy’s spectrum and its morphology. This is done by making use of an Artificial Neural Network, which is trained to identify galaxy morphology after being inputted with the galaxy spectra (from the first nine PCA eigenspectra).

### 5.1 Brief description

An artificial Neural Network (ANN) is a mathematical construct originally designed to simulate the functioning of the brain (see e.g. Ripley 1996). The network itself is designed around a set of layers, consisting of input nodes, hidden nodes and output nodes. The connections between these nodes can be quite complex and in most instances all the nodes in a previous layer are connected to all the nodes in the next layer. Because of this complexity the ANN can train itself to recognise highly nonlinear relationships between the inputs and the outputs we desire.

Each connection between two nodes has an associated weight,  $u_{ij}$ . The total input to any given node is the sum of all the individual inputs weighted by  $u_{ij}$ . Each node takes this total input and applies a transfer function to it, before passing it on to the next node. The transfer function is generally taken to be a sigmoid function,

$$f(z) = \frac{1}{1 + \exp(-z)}, \quad (10)$$

since this keeps the output in the range [0,1], hence limiting the variation in the possible weighting schemes.

In order to train the network we need to establish a cost function. This is usually taken to be the Euclidean separation between the desired outputs,  $T_i$ , we hope to receive (at each of our output nodes), and the actual outputs,  $F(\mathbf{u}, x_i)$ ,

$$E = \frac{1}{2} \sum_{i=1}^N [T_i - F(\mathbf{u}, x_i)]^2 \quad (11)$$

All the weights in our network are initially set to random values. The network is then trained on our training data-set by inputting the first four principal components and comparing the output to the desired morphology of each object. The weights are adjusted by means of back-propagation until a global minimum in the cost function is found. The network is then fully trained and can be run on the testing set to establish its success.

Another aspect of neural networks is that of weight decay, whereby one can specify an additional factor in the cost function in order to restrain the magnitude of the weights. We do not make use of this refinement for the following reason: If one specifies multiple outputs for the neural network (in our case two outputs, corresponding to Early and Late) these can in fact be interpreted as the probabilities that a galaxy belongs to either class - so long as the weight decay is set to 0.

Further details about the mathematical formulation and interpretation of ANNs is given in e.g. Lahav et al. (1996) and Bishop (1995).

### 5.2 Results from the ANN

The ANN was run using three different configurations, all of which had 9 inputs and 2 outputs, and as such were only distinguished by the structure and size of their hidden layers. The first network used had a single hidden layer of 5 nodes (configuration 9:5:2), the second increased this to 9 nodes (configuration 9:9:2), and the final ANN had two hidden layers with 5 nodes each (configuration 9:5:5:2).

In each case the network required both a ‘training’ and a ‘testing’ data set. Because there were so many more Late than Early type galaxies in our sample (2631 versus 1268 respectively), 800 of each type were randomly selected for the purposes of training. The reason that equal numbers of each type were used for training the ANN was because ANNs are essentially complicated Bayesian classifiers, as such the detection of each type will be biased by the prior distributional information of that type, which is determined by the selection criteria of the redshift survey. By using equal numbers of each type of galaxy in our training set we ensure that the results presented here are general and not only applicable to  $b_J$ -selected galaxy samples, which are biased towards recently star-forming galaxies.

The remaining 2299 galaxies were used as a testing and validating set. The purpose of validation is to ensure that the ANN does not ‘over-train’ on the training set by over-fitting the data which

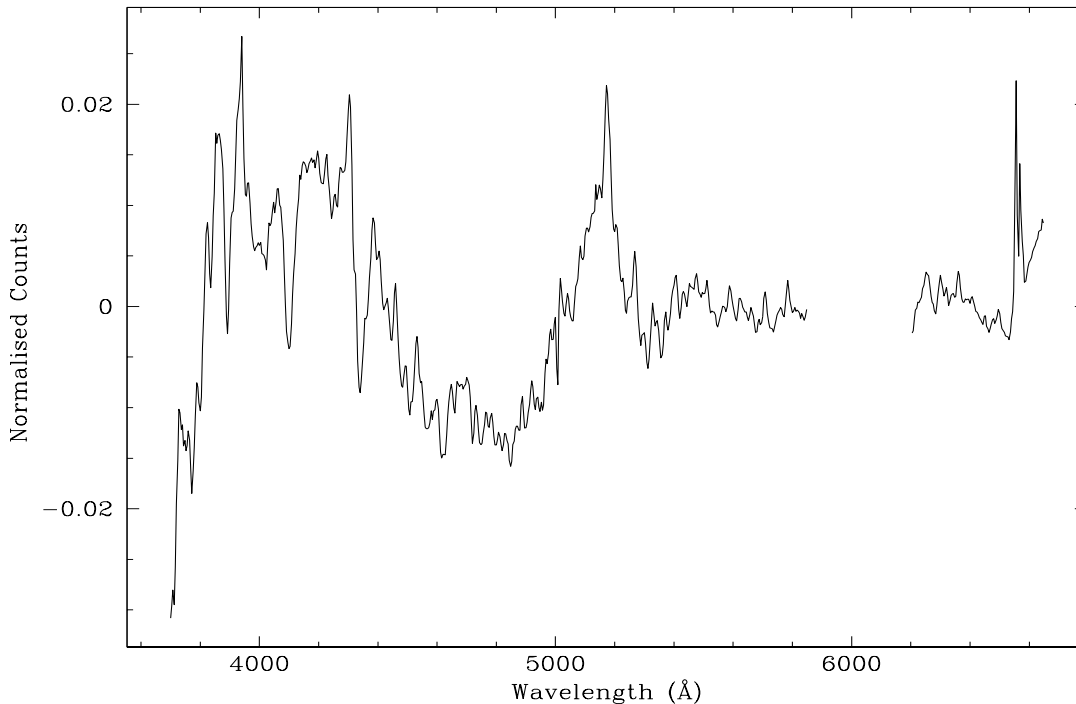


**Figure 9.** The combined 2dFGRS eigenspectrum corresponding to the Fisher criterion derived for determining galaxy morphology. It can be shown that the Fisher method is almost exclusively quantifying the magnitude of the 4000Å break, and that the entire classification can be created using only the part of this spectrum at wavelengths below 4800Å. The broad feature at  $\sim 5200\text{\AA}$  (corresponding to Mgb) is erroneous, and has resulted from the fact that we have truncated the series of eigenspectra just as this feature was becoming prominent.

it is supplied. For this reason the minimum in the error function (Eqn. 11) is calculated from the testing data set, rather than the training set. Note that for our purposes a galaxy was classified as Early type if the output probability from the ANN from the Early type node was greater than 0.5, and likewise for Late types.

In general it was found that the results were relatively insensitive to the choice of network architecture (changing by only a few percentage points of successfully detected galaxies of each type). This is consistent with the results from the previous section where it was found that the PCA eigenspectra generally carry the same physical information as each other - despite being ‘statistically’ independent.

The results from each ANN are summarised in Table. 2, and once again the  $(pc_1, pc_2)$  components are shown for the galaxies which have been classified by the ANN (in this case the 9:9:2 configuration) in Fig. 10. Again it can be seen that the classification can be quite accurately expressed using only these first two projections. The correspondence with the 2dFGRS  $\eta$  classification is also shown.

One problem that arose when attempting to separate the Early type galaxies in our sample was that we obtained a significant contamination from Late type galaxies ( $\sim 50\%$ ). It was found that this fractional contamination could be reduced somewhat by increasing the complexity of the ANN, however this resulted in a lower percentage of the actual Early type galaxies being correctly classified. The actual degree of this contamination will vary according to the galaxy population under consideration. In the case of the 2dFGRS we are presented with a  $b_J$ -selected sample of galaxies and as such there is a significantly higher proportion of Late type (star-

**Table 2.** Success rates of the ANNs. The numbers given are percentages of galaxies correctly classified for each morphological type.

Network	Configuration	Early	Late
1	9:5:2	67%	80%
2	9:9:2	70%	82%
3	9:5:5:2	67%	83%

forming) galaxies than Early types. On the other hand, in the case of a 2MASS (Jarrett et al. 2000) near-infrared selected galaxy sample, the proportion of types is reversed (Madgwick & Lahav 2001) and so a more pure sample of Early types can be determined.

## 6 APERTURE EFFECTS

Because our sample of morphologically classified galaxies is drawn from only the most nearby (and hence the most extended on the sky) galaxies, we must consider the possibility that the observed spectra are not representative of the galaxies as a whole. For example, the 2dF fibre (diameter 2-2.16”) may only sample the light from the bulge of a nearby spiral galaxy - the spectrum from which tends to be more similar to that of an Early type galaxy.

In order to test the importance of redshift upon the success of our morphological classifier we return to our ANN (configuration 9:9:2), trained previously. If aperture effects are important then we would expect to see that the ANN will recover the galaxy morphology of relatively distant galaxies more accurately than for nearby

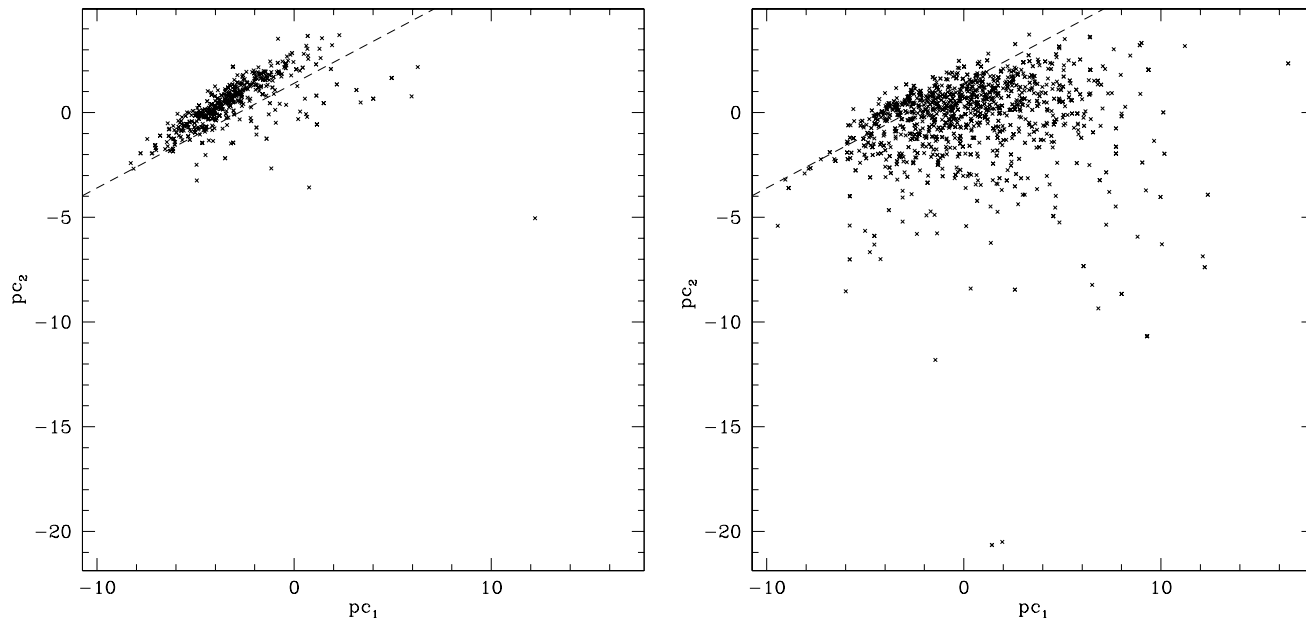


**Figure 10.** The  $pc_1$  and  $pc_2$  projections of the morphologically classified 2dFGRS galaxies are shown. Here the morphologies have been derived using an Artificial Neural Network with 9 principal components as inputs (9:9:2). Again we can see that all the information in these 9 components is essentially contained in just these first two projections.

galaxies, particularly in the case of Late type galaxies. For this reason the results from the previous section were re-determined after dividing the testing sample into two redshift bins,  $z < 0.05$  (1533 galaxies) and  $z > 0.05$  (761 galaxies).

The results are summarised in Table. 3. Contrary to our expectations the success of the classification is relatively immune to the redshift being sampled. Clearly the situation must be more complex than a simple analysis such as this can resolve.

One important aspect of the spectra being used in this analysis which may explain this situation is the substantial seeing present at the Anglo-Australian Telescope site. This seeing acts to ‘smooth out’ any spectral gradients which may be present in a given galaxy. In general the seeing is of the order of 1.8-2.5'' and so can effectively double the area being sampled by the 2dF fibre aperture.

Another major consideration in an analysis such as this is the stability of the morphological classification with redshift - as more distant galaxies will tend to be fainter and less extended on the sky. In general the robustness of a morphological classification is difficult to assess because of its subjectivity. It has been found in previous work (Naim et al. 1995) that this subjective element results in an uncertainty of the order of 2 T-Types. However, this figure does not incorporate the uncertainties introduced to the classification through inclination, obscuration and other systematic uncertainties. All of these uncertainties add to the importance of being able to estimate morphologies in a more robust manner such as by correlating with galaxy spectra, or indeed for neglecting morphology altogether and simply using a spectral-based classification (see e.g. Madgwick & Lahav 2001).

Because the galaxy sample considered here has been restricted to apparent magnitudes greater than  $b_J = 16.5$ , misclassification is not considered to be as significant an issue in this analysis as it might otherwise be. However when repeating the above analysis using galaxies fainter than this magnitude limit a very substantial

**Table 3.** Success rates of the 9:9:2 ANN for different redshift slices in the testing data set. The numbers given are percentages of correctly classified galaxies of each specified morphological type.

Redshift	$N_{\text{tot}}$	Early	Late
$z < 0.05$	1533	72%	82%
$z > 0.05$	761	67%	82%

systematic misclassification of spirals was observed. This was to be expected since the spiral arms of such galaxies will become more difficult to resolve at higher redshift (where most of the faintest galaxies will reside), particularly for galaxies inclined to the line-of-sight.

## 7 DISCUSSION

Perhaps one of the most interesting aspects of this work on recovering galaxy morphologies from their spectra, is how closely related the results from advanced statistical methods appear to be to the original 2dFGRS spectral classification,  $\eta$ . In some regards this was to be expected, since one is always inclined to relate one’s classification to galaxy morphology during its derivation. For example Folkes et al. (1999) used a training set of 26 galaxies drawn from the Kennicutt Atlas (Kennicutt 1992) as a training set to derive the original 2dFGRS spectral classification. These 26 galaxies were ‘projected’ onto the  $(pc_1, pc_2)$  plane defined by the 2dFGRS spectra and lines were drawn by-hand to roughly separate the galaxies according to their assumed morphologies. However, in the case of  $\eta$  this method was not used, rather the galaxies were classified solely on the basis of finding the most statistically significant projection in

the PCA which was robust to the known instrumental uncertainties in the 2dF instrument (see Madgwick et al. 2002 for more details).

The overall success of correlating galaxy morphologies and spectra, using the methods considered in this paper, is summarised in Fig. 11, where the percentages of galaxies classified correctly is shown for each method. In the case of the  $\eta$  spectral classification and the Fisher discriminant it is possible to change the relative success rates between types simply by adopting different ‘cuts’ in these continuous parameters. This is demonstrated in Fig. 11 where the success rates are shown for both an  $\eta < -1.4$  cut (2dFGRS default) and an  $\eta < -2.0$  cut.

In general, the most successful method of correlating galaxy morphology with spectra appears to be the Artificial Neural Network, which can achieve consistently high success rates for both types of galaxies. However, in deciding whether to implement such an algorithm the relative pay-off must be weighed against the additional complexity of this algorithm. This is particularly true for this data-set since all three methods of classification make roughly similar distinctions between morphological types. However, with the advent of higher resolution (and signal-to-noise) spectra, it is possible that such advanced methods will become much more successful.

Note that in practical situations the interpretation of Fig. 11 is not as straight-forward as it might at first seem. One must also bear in mind the relative fractions of different galaxy types in the sample under consideration. In the case of the 2dFGRS, there are over 2 times as many Late type galaxies as Early types (2610 and 1289 galaxies respectively), so a decrease in the success rate of classifying Late types by 5% implies there will be an additional 250 galaxies classified as Early type, which is at least a 10% contamination of the Early type sample. This is particularly important if one wants to create a relatively ‘pure’ sample of a particular type of galaxy (e.g. for efficient use of telescope time during observational follow-ups).

## 8 CONCLUSIONS

Establishing a firm link between a galaxy’s morphology and its spectrum is advantageous for several reasons. For instance, galaxy spectra can be accurately determined to much greater redshifts and for fainter objects than morphologies. Also, most large redshift surveys currently taking place will contain many thousands of galaxy spectra but little information relating to the optical morphologies of those galaxies. In particular the separation of different morphological types of galaxies in these redshift surveys will be very useful as a means of separating objects for follow-up observations to determine independent distance measurements using either  $D_n - \sigma$  or the Tully-Fisher relation.

In this paper I have tried to quantify the link between galaxy spectra and morphology using several advanced statistical methods; namely, Fisher’s linear discriminant and Artificial Neural Networks. The best results produced suggest that it is possible to use optical galaxy spectra to create galaxy samples containing 70% of the Early type galaxies present and 80% of the Late types respectively. The contamination between these samples depends on the morphological mix of the survey under consideration. In the case of the  $b_J$ -selected 2dFGRS the most significant contamination will be of mis-classified Late types in the Early type sample ( $\sim 40\%$  contamination), in the case of a near-infrared selected sample this situation will be reversed.

Essentially the results obtained using more advanced statistical techniques (Sections 4 and 5) are comparable to those that

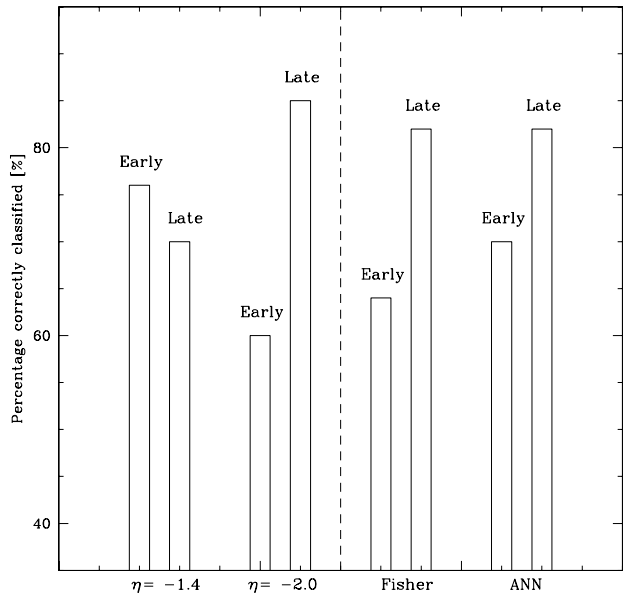


**Figure 11.** Comparison between the success rates of different classification methods. The first two sets of histograms show the success rates that can be achieved simply by using the (PCA based)  $\eta$  spectral classification adopted in the 2dFGRS. The second two histograms show the success rates for the more advanced statistical methods: Fisher’s linear discriminant and the ANN. It can be seen that the results are generally comparable, although the ANN gives the best results.

could be obtained simply using the default 2dFGRS spectral classification  $\eta$  (Madgwick et al. 2002) which can be accessed from the 2dFGRS database<sup>2</sup>. This is an interesting result and certainly adds significantly to the physical interpretation of this parameter.

Another interesting aspect of this analysis is that the Fisher discriminant (Section 4) identified the 4000Å break to be the most essential element of a galaxy’s spectrum for the purposes of estimating its morphology. This result is somewhat expected since the general correlation between galaxy morphology and colour is already well established. However, it is intriguing to see this result derived in a quantitative manner from the observed spectra themselves.

The results presented in this paper are essentially limited by the coarseness of the morphological classification adopted, which for practical reasons can only be divided into two separate types (rather than a more realistic sequence of types). As larger samples of more accurately morphologically classified galaxies become available it will be interesting to repeat the analysis presented here, in order to determine whether even more information can be recovered to link a galaxy’s morphology and spectrum.

## ACKNOWLEDGMENTS

I wish to thank Ofer Lahav for suggesting this project and providing plenty of invaluable advice and suggestions. Raven Kaldare and Andrew Firth were very helpful in explaining the intricacies of Artificial Neural Networks to me. I would also like to thank the

<sup>2</sup> Spectral extension parameter ETA\_TYPE

anonymous referee for their helpful comments on the draft of this paper. The efforts of the 2dFGRS collaboration, in preparing and compiling the data used in this analysis, are greatly appreciated. This work was supported by an Isaac Newton studentship from the Institute of Astronomy and Trinity College, Cambridge.

## REFERENCES

- Bishop C., 1995, *Neural Networks for Pattern Recognition*, Oxford University Press
- Colless, M. M., et al., 2001, *MNRAS*, 328, 1039
- Connolly A.J., Szalay A.S., Bershady M.A., Kinney A.L., Calzetti D., 1995, *AJ*, 110, 1071
- Dressler A., et al., 1987, *ApJ*, 313, 42
- Folkes S.R., Lahav O., Maddox S.J., 1996, *MNRAS*, 283, 651
- Folkes S., et al. (the 2dFGRS Team), 1999, *MNRAS*, 308, 459
- Galaz G., de Lapparent V., 1998, *A&A*, 332, 459
- Jarrett T. H., et al., 2000, *AJ*, 119, 2498
- Hambly N., et al., 2001, *MNRAS*, 326, 1279
- Hubble E. P., 1936, *The Realm of the Nebulae*, Yale University Press
- Kennicutt R.C., Jr., 1992, *ApJS*, 79, 255
- Kochanek C.S., Pahre M.A., Falco E.E., 2000, *ApJ* submitted (astro-ph/0011458)
- Lahav O., Naim A., Sodre L., Storrie-Lombardi M. C., 1996, *MNRAS*, 283, 207
- Lewis I., et al., 2002, *MNRAS*, in press (astro-ph/0202175)
- Loveday J., 1996, *MNRAS*, 278, 1025
- Maddox S. J., Sutherland W. J., Efstathiou G., Loveday J., 1990a, *MNRAS*, 243, 692
- Maddox S. J., Efstathiou G., Sutherland W. J., 1990b, *MNRAS*, 246, 433
- Madgwick D. S., et al., 2002, *MNRAS*, 333, 133
- Madgwick D. S., Lahav O., 2001, To appear in 'Where's the Matter? Tracing Dark and Bright Matter with the New Generation of Large Surveys', Treyer & Tresse Eds, Fronteir Group
- Morgan W. W., Mayall N. U., 1957, *PASP*, 69, 291
- Murtagh F., Heck A., 1987, *Multivariate Data Analysis*. Riedel, Dordrecht
- Naim A., et al., 1995, *MNRAS*, 274, 1107
- Ripley B. D., 1996, *Pattern Recognition and Neural Networks*, Oxford University Press
- Tully R. B., Fisher J. R., 1977, *A&A*, 54, 661
- York D. G., et al., 2000, *AJ*, 120, 1579

This paper has been typeset from a  $\text{\TeX}$ / $\text{\LaTeX}$  file prepared by the author.